

Proceedings of XIX International Scientific Conference “New Technologies and Achievements in Metallurgy, Material Engineering, Production Engineering and Physics”, Częstochowa, Poland, June 7–8, 2018

The Evolution of Phase Constitution and Magnetic Properties of the Annealed Pr–Fe–B–W Alloy Ribbons

K. FILIPECKA^{a,b}, P. PAWLIK^{a,*}, A. KOZDRAŚ^c, J. FILIPECKI^b AND K. PAWLIK^a

^aInstitute of Physics, Faculty of Production Engineering and Materials Technology,
Częstochowa University of Technology, al. Armii Krajowej 19, 42-200 Częstochowa, Poland

^bInstitute of Physics, Faculty of Mathematics and Natural Science, Jan Długosz University,
al. Armii Krajowej 13/15, 42-200 Częstochowa, Poland

^cDepartment of Physics, Faculty of Production Engineering and Logistics, Opole University of Technology,
Ozimska 75, 45-370 Opole, Poland

In the present studies the influence of annealing conditions on the phase constitution and magnetic properties of the rapidly solidified Pr₉Fe₆₅W₈B₁₈ alloy ribbon samples was analyzed. The base alloy was obtained by the arc-melting of the high purity constituent elements under a low pressure of Ar protective atmosphere. The thick ribbon samples ($t \approx 70 \mu\text{m}$) were produced by the single-roll melt spinning technique under the low argon pressure at the linear velocity of the copper roll surface of 6 m/s. The X-ray diffraction studies have shown amorphous structure of as-cast ribbons. Heat treatment carried out at various temperatures (from 923 K to 1023 K) caused changes in the magnetic properties of the alloy. The X-ray diffraction studies revealed evolution of the phase constitution of annealed ribbons. The phase analysis has shown presence of hard magnetic Pr₂Fe₁₄B and paramagnetic Pr_{1+x}Fe₄B₄ phases.

DOI: [10.12693/APhysPolA.135.226](https://doi.org/10.12693/APhysPolA.135.226)

PACS/topics: 75.50.Ww, 75.50.Kj, 71.20.Eh

1. Introduction

The RE–Fe–B-type permanent magnets play a significant role in the global market of hard magnetic materials. The biggest advantage of these materials in comparison to other magnets are higher values of magnetic parameters, such as the coercivity field JH_c and the maximum magnetic energy product $(BH)_{\text{max}}$. The most widely used magnets are Nd–Fe–B alloys. However, in recent years a lot of attention has been focused on Pr–Fe–B magnets due to the possibility of their application at low temperatures [1]. Here the Pr₂Fe₁₄B phase is responsible for their good magnetic properties [2]. This phase has higher value of the anisotropy field (87 kOe) than that obtained for the Nd₂Fe₁₄B (67 kOe) counterpart [3], thus a higher value of coercivity field JH_c is expected. A numerous studies have been carried out in order to determine the influence of basic components (Pr, Fe, B) [4, 5] and admixture of other elements [6–9] on magnetic properties and microstructure of the Pr–Fe–B-base materials. On the other hand, the magnetic parameters strongly depend on the production technology. Rapid solidification technique leading to formation of the amorphous phase allows to obtain nanocrystalline structure and hard magnetic properties by controlled heat treatment. Furthermore,

the application of rapid solidification processes leads to reduction of the manufacturing costs. Price of Pr–Fe–B-type magnets can be further reduced for alloys of lower Pr concentration. For this purpose the studies of evolution of the phase constitution and magnetic properties of the rapidly solidified Pr₉Fe₆₅W₄B₂₂ alloy ribbons subjected to annealing were performed.

2. Experimental

The Pr₉Fe₆₅W₈B₁₈ base alloy was prepared by arc-melting of the high purity elements under an inert gas atmosphere (Ar). The ingot was homogenized by its multiple re-melting. The ribbon specimens were produced by melt-spinning technique under the argon atmosphere at constant velocity of the copper roll surface of 6 m/s. The alloy ribbons were sealed-off in a quartz tube under a low pressure of Ar (0.5 bar) and subjected to annealing at temperatures ranging from 923 K to 1023 K for 5 min and subsequently quenched in water. The crystallization behavior of the samples was analyzed by the differential scanning calorimeter Netzsch DSC404 at a heating rate of 10 K/min. The phase structure was studied using the Bruker D8 Advance diffractometer with Cu K_α radiation and LynxEye 1-D energy-dispersive detector. Magnetic properties were examined using LakeShore 7307 vibrating sample magnetometer at external magnetic fields up to 2 T at room temperature.

*corresponding author; e-mail: pawlik@wip.pcz.pl

3. Results and discussion

The DSC scan measured for the amorphous as-cast ribbon sample was shown in Fig. 1. It was revealed that the crystallization process proceeds through two steps corresponding to exothermic peaks on DSC curve. The crystallization temperatures T_{x_1} of 920 K and T_{x_2} of 1020 K were determined from this curve. Base on these results, the range of annealing temperatures (at which crystallization of hard magnetic phase occurs) was specified.

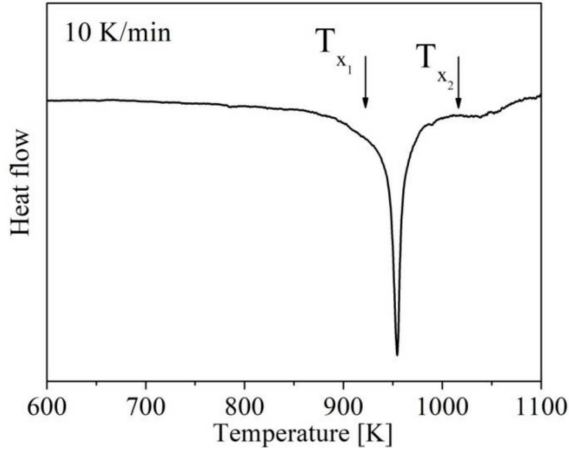


Fig. 1. DSC curves obtained for rapidly solidified $\text{Fe}_{65}\text{Pr}_9\text{B}_{18}\text{W}_8$ ribbon measured at a heating rate of 10 K/min.

The XRD scans measured for the $\text{Fe}_{65}\text{Pr}_9\text{B}_{18}\text{W}_8$ alloy ribbons in the as-cast state and those annealed at temperatures ranging from 923 K to 1023 K for 5 min are presented in Fig. 2. For as-cast sample a wide bump on XRD pattern in the range of 2θ from 35 to 50 deg, characteristic for the amorphous phase, was observed. For ribbon annealed at 923 K except the halo corresponding to the amorphous phase, reflexes coming from crystalline phases were detected. The XRD phase analysis carried out for this sample suggests a presence of hard magnetic $\text{Pr}_2\text{Fe}_{14}\text{B}$ phase based on positions of major identified peaks. However, intensities of those peaks are different than those measured for samples annealed at higher temperatures. This might be related to different orientation of precipitating crystallites formed during annealing at 923 K. However, further studies have to be done to confirm this fact. Furthermore, a peak present at ≈ 45 deg was not properly identified, that may suggest that it corresponds to some metastable phase formed at this temperature. Heat treatment of specimens at the 943 K and higher temperatures led to nucleation and growth of crystalline phases and allowed to obtain a nanocrystalline structure. The XRD traces have shown changes of peak intensities for samples annealed at higher temperatures. The phase analysis indicates a presence of the hard magnetic $\text{Pr}_2\text{Fe}_{14}\text{B}$ and the paramagnetic $\text{Pr}_{1+x}\text{Fe}_4\text{B}_4$ phases.

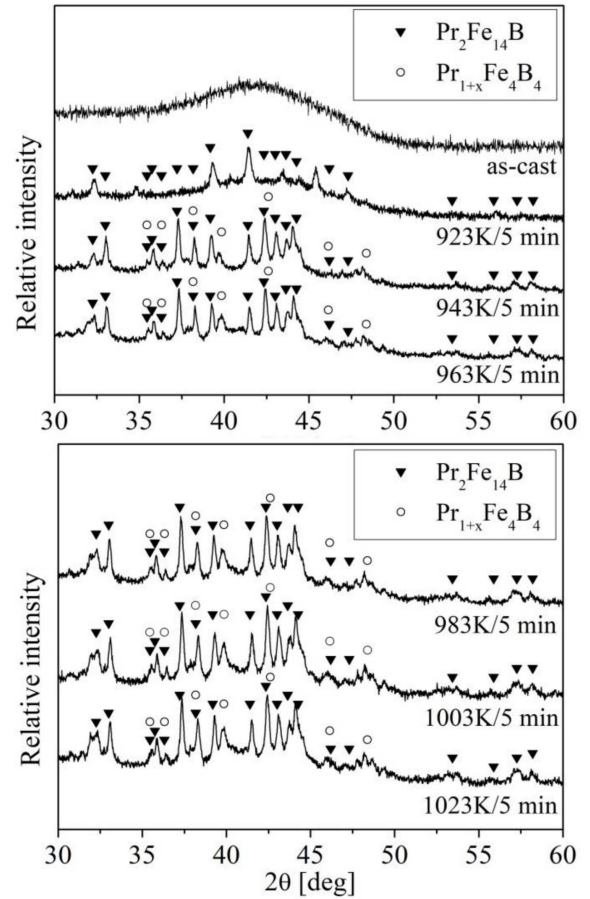


Fig. 2. The X-ray diffraction patterns for the rapidly solidified $\text{Fe}_{65}\text{Pr}_9\text{B}_{18}\text{W}_8$ alloy ribbons in as-cast state and subjected to annealing at various temperatures for 5 min.

TABLE I

Magnetic parameters: coercivity field JH_c , remanence polarization J_r and maximum energy product $(BH)_{\max}$ for annealed ribbon samples.

Annealing temperature [K]	JH_c [kA/m]	J_r [T]	$(BH)_{\max}$ [kJ/m ³]
943	951	0.39	23
963	944	0.40	26
983	1009	0.37	24
1003	1065	0.39	27
1023	1058	0.34	21

The hysteresis loops measured for the $\text{Fe}_{65}\text{Pr}_9\text{B}_{18}\text{W}_8$ alloy ribbons in as-cast state and those subjected to annealing at temperatures ranging from 923 K to 1023 K for 5 min are shown in Fig. 3. Magnetic measurements carried out on as-cast ribbon have shown its soft magnetic properties. Similar shape of hysteresis loop was measured for the sample subjected to annealing at 923 K, proving precipitation of low volume fraction of crystalline phases within the amorphous matrix. Increase of annealing temperature caused the evolution

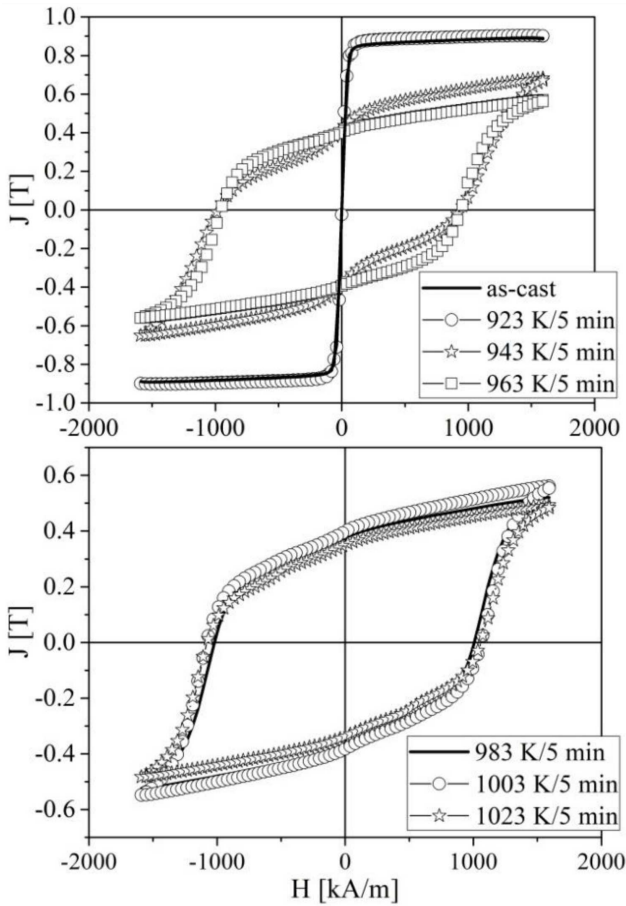


Fig. 3. The hysteresis loops measured for rapidly solidified $\text{Fe}_{65}\text{Pr}_9\text{B}_{18}\text{W}_8$ alloy ribbons in as-cast state and subjected to annealing at various temperatures for 5 min.

of microstructure and phase constitution, which resulted in hard magnetic properties of the samples. The basic magnetic parameters of the annealed $\text{Fe}_{65}\text{Pr}_9\text{B}_{18}\text{W}_8$ alloy ribbons were collected in Table I. With the increase of annealing temperatures, an increase of the coercivity was observed. The maximum value of the coercivity field $JH_c = 1065 \text{ kA/m}$ and the maximum magnetic energy product $(BH)_{\max} = 27 \text{ kJ/m}^3$ were measured for the ribbon annealed at 1003 K for 5 min. Large volume fraction of the paramagnetic $\text{Pr}_{1+x}\text{Fe}_4\text{B}_4$ phase and change of the chemical composition of the amorphous matrix resulted in relatively low values of $(BH)_{\max}$. Annealing

at 1023 K resulted in slight deterioration of the magnetic properties, which might be related to the crystallization of an additional phase (indicated by the DSC measurements) accompanied by reduction of volume fraction of the hard magnetic phase.

4. Conclusions

The melt-spun $\text{Fe}_{65}\text{Pr}_9\text{B}_{18}\text{W}_8$ alloy ribbon in as-cast state had amorphous structure and revealed soft magnetic properties. XRD studies of ribbon annealed at 923 K for 5 min have shown that next to the amorphous phase, diffraction peaks coming from the hard magnetic $\text{Pr}_2\text{Fe}_{14}\text{B}$ and other unidentified phase were observed. However, a low fraction of those phases did not cause changes in the magnetic properties of the ribbon. Annealing at 943 K and higher temperatures led to the nucleation and growth of the hard magnetic $\text{Pr}_2\text{Fe}_{14}\text{B}$ and paramagnetic $\text{Pr}_{1+x}\text{Fe}_4\text{B}_4$ crystalline phases. Moreover, with increase of the annealing temperature an increase of magnetic parameters was observed. The maximum values of these parameters were obtained in the sample annealed at 1003 K for 5 min.

References

- [1] Z. Liu, H.A. Davies, *IEEE Trans. Magn.* **40**, 2898 (2004).
- [2] J.H. Herbst, W.B. Yelon, *J. Appl. Phys.* **57**, 2343 (1985).
- [3] S. Hirose, Y. Matsuura, H. Yamamoto, *J. Appl. Phys.* **59**, 873 (1986).
- [4] H.W. Chang, W.C. Chang, Z.Y. Pang, S.H. Han, B.S. Han, *J. Magn. Magn. Mater.* **279**, 149 (2004).
- [5] C. You, N. Tian, Z. Lu, L. Ge, X. Jing, *Acta Metall. Sin. (English)* **23**, 321 (2010).
- [6] H.W. Chang, C.H. Chiu, C.W. Chang, C.H. Chen, W.C. Chang, A.C. Sun, Y.D. Yao, *J. Magn. Magn. Mater.* **304**, 216 (2006).
- [7] M. Szwaja, P. Gebara, J. Filipecki, K. Pawlik, A. Przybył, P. Pawlik, J.J. Wysłocki, K. Filipecka, *J. Magn. Magn. Mater.* **382**, 307 (2015).
- [8] K. Filipecka, P. Pawlik, J. Filipecki, *J. Alloys Comp.* **694**, 228 (2017).
- [9] Z.C. Wang, H.A. Davies, *Mater. Sci. Eng. A* **375-377**, 1157 (2004).